Biochimica et Biophysica Acta 1853 (2015) 619–631

Contents lists available at ScienceDirect

Biochimica et Biophysica Acta

journal homepage: www.elsevier.com/locate/bbamcr

Cystamine induces AIF-mediated apoptosis through glutathione depletion

Sung-Yup Cho [a,1], Jin-Haeng Lee [a,1], Mi-kyeong Ju [a], Eui Man Jeong [a,b], Hyo-Jun Kim [a], Jisun Lim [a], Seungun Lee [a], Nam-Hyuk Cho [c], Hyun Ho Park [d], Kihang Choi [e], Ju-Hong Jeon [b,f], In-Gyu Kim [a,b,*]

[a] Department of Biochemistry and Molecular Biology, Seoul National University College of Medicine, Seoul 110-799, Republic of Korea
[b] Institute of Human–Environment Interface Biology, Seoul National University College of Medicine, Seoul 110-799, Republic of Korea
[c] Department of Microbiology and Immunology, Seoul National University College of Medicine, Seoul 110-799, Republic of Korea
[d] Graduate School of Biochemistry, Yeungnam University, Gyeongsan 712-749, Republic of Korea
[e] Department of Chemistry, Korea University, Seoul 136-701, Republic of Korea
[f] Department of Physiology and Biomedical Sciences, Seoul National University College of Medicine, Seoul 110-799, Republic of Korea

ARTICLE INFO

Article history:
Received 22 August 2014
Received in revised form 9 December 2014
Accepted 22 December 2014
Available online 27 December 2014

Keywords:
Apoptosis-inducing factor
Nuclear translocation
Caspase-independent cell death
Glutathione
Cystamine
Cysteamine

ABSTRACT

Cystamine and its reduced form cysteamine showed protective effects in various models of neurodegenerative disease, including Huntington's disease and Parkinson's disease. Other lines of evidence demonstrated the cytotoxic effect of cysteamine on duodenal mucosa leading to ulcer development. However, the mechanism for cystamine cytotoxicity remains poorly understood. Here, we report a new pathway in which cystamine induces apoptosis by targeting apoptosis-inducing factor (AIF). By screening of various cell lines, we observed that cystamine and cysteamine induce cell death in a cell type-specific manner. Comparison between cystamine-sensitive and cystamine-resistant cell lines revealed that cystamine cytotoxicity is not associated with unfolded protein response, reactive oxygen species generation and transglutaminase or caspase activity; rather, it is associated with the ability of cystamine to trigger AIF nuclear translocation. In cystamine-sensitive cells, cystamine suppresses the levels of intracellular glutathione by inhibiting γ-glutamylcysteine synthetase expression that triggers AIF translocation. Conversely, glutathione supplementation completely prevents cystamine-induced AIF translocation and apoptosis. In rats, cysteamine administration induces glutathione depletion and AIF translocation leading to apoptosis of duodenal epithelium. These results indicate that AIF translocation through glutathione depletion is the molecular mechanism of cystamine toxicity, and provide important implications for cystamine in the neurodegenerative disease therapeutics as well as in the regulation of AIF-mediated cell death.

1. Introduction

Cystamine is a disulfide amine that has antioxidative capacity and alters cellular antioxidant system [1–3]. Under intracellular conditions, cystamine is in equilibrium with its reduced form cysteamine which has a direct antioxidant effect [4–6]. In neuronal tissue, cystamine protected against cell death in several disease models that are thought to be associated with oxidative stress, including Huntington's disease [7,8], Parkinson's disease [9,10], dentatorubral-pallidoluysian atrophy [11] and neuropsychiatric systemic lupus erythematosus [12]. Thus, therapeutic effect of cysteamine for patients with Huntington's disease has been tested in clinical trial [13]. In addition to the role of cystamine as an antioxidant, other mechanisms have been proposed for its neuroprotective effect. It has been shown that cystamine modulates the apoptotic process by inhibition of enzymes such as caspase-3 and transglutaminases [3,5,14]. Moreover, cystamine is also involved in the regulation of cellular responsiveness to oxidative stress. It has been reported that cystamine increases the expression levels of heat-shock protein [8], brain-derived neurotrophic factor [15] and glutathione transferase A3 [16]. These observations indicate that cystamine directly or indirectly suppresses oxidative stress-induced neuronal cell death.

However, other lines of evidence demonstrated that cystamine promotes oxidative stress-induced cell death in other type of cells, especially in intestinal epithelium, by inhibition of γ-glutamylcysteine

Abbreviations: AIF, apoptosis-inducing factor; BP, 5-biotinamidopentylamine; BSA, bovine serum albumin; BSO, buthionine sulfoximine; DCF, dichlorofluorescein; DPQ, 3,4-dihydro-5-[4-(1-piperidinyl)butoxy]-1(2H)-isoquinolinone; DTNB, 5,5′-dithio-bis-2-nitrobenzoic acid; DTT, dithiothreitol; GCS, γ-glutamylcysteine synthetase; GSH, glutathione; GSH-EE, glutathione ethyl ester; *Hq*, *Harlequin*; MAPK, mitogen-activated protein kinase; NAC, N-acetylcysteine; PBS, phosphate buffered saline; PARP-1, poly (ADP-ribose) polymerase-1; ROS, reactive oxygen species; TG2, transglutaminase 2; TNB, 5-thio-2-nitrobenzoic acid; TRAIL, tumor necrosis factor-related apoptosis-inducing ligand; UV, ultraviolet; β-ME, β-mercaptoethanol

* Corresponding author at: Department of Biochemistry and Molecular Biology, Seoul National University College of Medicine, 103 Daehak-ro, Jongno-Gu, Seoul 110-799, Republic of Korea. Tel.: +82 2 740 8248; fax: +82 2 744 4534.
E-mail address: igkim@snu.ac.kr (I.-G. Kim).
[1] These authors contributed equally.

http://dx.doi.org/10.1016/j.bbamcr.2014.12.028
0167-4889/

synthetase (GCS), a key enzyme for glutathione (GSH) synthesis [2,17]. Cystamine is known to inhibit GCS through a sulfhydryl–disulfide interchange reaction between sulfhydryl groups at or around the active site of the GCS and cystamine [6], and the reduced form cysteamine also acts as a competitive inhibitor [5]. Indeed, Vanin-1, a cysteamine synthesizing enzyme, deficient mice showed no detectable free cysteamine and increased levels of intracellular GSH in intestinal epithelium [18,19]. Consequently, these mice were resistant to oxidative stress and inflammation, and deficient phenotypes were reversed by cystamine administration [6,19]. Moreover, cysteamine administration induces cell death of duodenal mucosal cells [20], possibly by generating hydrogen peroxides [19], resulting in perforating ulcers in rat. This rat model of cysteamine-induced duodenal ulcer is easily reproducible and similar to human duodenal ulcer, and thus has been used for studying the pathogenesis of duodenal ulceration. The concentration of cysteamine used in rat duodenal ulcer model (intragastric, 250 mg/kg three times at 4 h intervals) was similar to the concentration of cystamine in mouse neurodegenerative disease models (intraperitoneally, 100–750 mg/kg) [7,9,20]. These observations indicate that the effect of cystamine on cell survival is partly dependent on cell-type, and that investigation on the mechanism for cystamine cytotoxicity is needed for re-evaluating cystamine as a new medication for neurodegenerative diseases as well as for better understanding of the etiology of duodenal ulceration.

GSH is the most important non-protein antioxidant and has a critical role in maintaining cellular redox status. Under physiological conditions, intracellular GSH concentrations range from 1 to 11 mM. Although GCS expression and activity is tightly regulated at different levels to maintain GSH concentration [21], GSH is depleted by increased oxidative stress or treatment with apoptotic agents such as death receptor ligands or chemotherapeutics [22]. Thus, the level of intracellular GSH is considered to be a marker for cellular redox status during oxidative stress-induced cell death. However, it is also known that GSH depletion *per se* induces cell death. GCS deficient mice displayed embryonic lethality due to a massive cell death [23]. Pharmacological inhibition of GCS with buthionine sulfoximine (BSO) induces or stimulates cell death [24,25]. Moreover, GSH depletion is required for Fas ligand-induced apoptosis regardless of reactive oxygen species (ROS) generation and oxidative stress [26], suggesting a previously unidentified mechanism for oxidative stress-induced cell death.

Apoptosis-inducing factor (AIF) is a flavoprotein that is located in the mitochondrial intermembrane space and plays major roles in mediating caspase-independent cell death [27]. Upon cell death stimuli, AIF is cleaved within the mitochondria by calpains and cathepsins [28], released into cytosol possibly through a mitochondrial permeability transition pore, and translocated into the nucleus where it induces chromatin condensation and DNA fragmentation through complex formation with H2AX and cyclophilin A [29,30]. A number of apoptotic stimuli have been documented to induce AIF mitochondria-to-nucleus translocation including DNA damaging agents, hypoxia/ischemia, oxidative stress and excitotoxins such as glutamate [27]. However, the signaling pathways that cause AIF nuclear translocation have not been fully elucidated.

In this study, we examined the cystamine cytotoxicity in various tumor cell lines, and found that cystamine induces caspase-independent cell death in a cell-type specific manner. In cystamine-sensitive cell lines, cystamine causes the depletion of intracellular GSH which triggers AIF nuclear translocation. These results were verified in a rat model of cysteamine-induced duodenal ulcer.

2. Materials and methods

2.1. Cell culture

DU145, human prostate cancer cells and HeLa, human cervical cancer cells were maintained in Dulbecco's modified Eagle medium (WelGENE, Daegu, Korea) containing 10% heat-inactivated fetal bovine serum (Hyclone, Logan, UT, USA). The neuroblastoma cells, SK-N-SH and SH-SY-5Y were also cultured in Dulbecco's modified Eagle medium. MCF7, human breast cancer cells and A549, human lung cancer cells were maintained in RPMI 1640 medium (WelGENE) containing 10% heat-inactivated fetal bovine serum. Penicillin (100 U/ml; Invitrogen, Carlsbad, CA, USA), streptomycin sulfate (100 μg/ml; Invitrogen) and glutamine (2 mM; Invitrogen) were supplemented to all cell culture media. All cells were maintained in a humidified incubator with 5% CO_2 at 37 °C.

All cells were grown to 20% confluence and then treated with cystamine, cysteamine, dithiothreitol (DTT; ICN Biomedicals Inc., Aurora, OH, USA) or β-mercaptoethanol (β-ME; Merck, Darmstadt, Germany) for 72 h. Parallel groups of cells were pretreated with N-acetylcysteine (NAC), vitamin C, vitamin E, Trolox (6-hydroxy-2,5,7,8-tetramethylchroman-2-carboxylic acid), quercetin, glutathione ethyl ester (GSH-EE), BSO or z-VAD-fmk for 1 h prior to addition of cystamine or cysteamine. Cells were pretreated with polyethylene glycol (PEG)-conjugated catalase for 4 h. All chemicals were purchased from Sigma-Aldrich Corporation (St. Louis, MO, USA) unless otherwise indicated.

HeLa cell lines expressing shRNA of transglutaminase 2 (TG2; $HeLa^{shTG2}$) were established by transfection with pSUPER plasmid containing shRNA for TG2 as described previously [31]. For knock-down of AIF, HeLa cells were transfected with siRNA for AIF (Santa Cruz Biotechnology, Santa Cruz, CA, USA) using Lipofectamine 2000 (Invitrogen) according to the manufacturer's instructions. The expression of TG2 and AIF was confirmed by Western blot analysis.

2.2. MTT colorimetric assay

Cells were cultured to 20% confluence on 24-well dishes and treated with cystamine, cysteamine, DTT or β-ME for the indicated times. After washing with phosphate buffered saline (PBS), cells were incubated for 4 h in MTT solution (500 μg/ml of tetrazolium MTT (3-(4,5-dimethylthiazolyl-2)-2,5-diphenyltetrazolium bromide; Sigma-Aldrich Corporation) in culture medium). MTT solution was removed, and dimethyl sulfoxide (DMSO) was added to dissolve the formazan crystals. The 24-well dishes were slightly vortexed and incubated in the dark. Samples were diluted to proper concentration and transferred to a 96-well plate. The absorbance at 570 nm in each well was measured by a microplate spectrophotometer. Values for untreated controls were set at 100% cell viability, and each treatment was assessed as a percentage of the control values. Each treatment was performed in triplicate.

2.3. Lactate dehydrogenase release assay

Lactate dehydrogenase (LDH) released to culture medium was estimated using CytoTox 96 Non-radioactive Cytotoxicity Assay (Promega, Madison, WI, USA) according to the manufacturer's instruction. Cells were treated with cystamine or cysteamine for 72 h, and 50 μl of culture media was transferred to the 96-well plate. After the addition of 50 μl of LDH substrate reagent to each well, the plate was incubated for 30 min in the dark and 50 μl of stop solution was added. The absorbance at 490 nm was measured by the microplate spectrophotometer. The background values were subtracted, and each treatment was assessed as a percentage of the untreated control values. Each treatment was performed in triplicate.

2.4. In situ transglutaminase (TG) activity assay

Cells were incubated for 1 h with 1 mM 5-biotinamidopentylamine (BP; Pierce, Rockford, IL, USA) and harvested by centrifugation. The cells were ruptured by sonication, followed by centrifugation (14000 *g*, 10 min at 4 °C). The cellular proteins (10 μg/well) in coating buffer (50 mM Tris–Cl, pH 7.5, 150 mM NaCl, 5 mM EGTA, 5 mM

EDTA) were added to each well of a 96-well microtiter plate. *In situ* TG activity was estimated by measuring the amount of BP that is incorporated into the proteins. The BP-incorporated products were probed using horseradish peroxidase-conjugated streptavidin (Zymed Laboratories, South San Francisco, CA, USA) followed by a reaction with o-phenylenediamine dihydrochloride (Sigma-Aldrich Corporation). After incubation for 5 to 10 min at room temperature, the reaction was stopped by the addition of H_2SO_4. The absorbance at 490 nm was measured by the microplate spectrophotometer.

2.5. ROS detection using dichlorofluorescein (DCF)

For measurement of the ROS generation, cells were harvested by centrifugation and incubated with 40 μM DCF in KRH buffer (10 mM HEPES, pH 7.4, 150 mM NaCl, 6 mM KCl, 1 mM $MgCl_2$) containing 0.2% bovine serum albumin (BSA) and 1 μg/μl glucose for 30 min at 37 °C. After washing, cells were then analyzed by flow cytometry (Becton Dickinson, San Jose, CA, USA) with 488 nm excitation and 535 nm emission filters. Data analysis was performed using the ModFit LT V3.0 software (Verity Software House, Topsham, ME, USA).

2.6. Analysis of cellular DNA content by PI staining

Cells were treated with 500 μM cystamine for 72 h and were harvested by trypsinization. After washing with PBS, cells ($\sim 1 \times 10^6$) were fixed in 1 ml of 70% ethanol at 4 °C for overnight and resuspended in 200 μl of PBS containing 50 μg/ml propidium iodide and 100 μg/ml RNase A. After incubating for 30 min in the dark at room temperature, cells were then analyzed by flow cytometry (Becton Dickinson) with 488 nm excitation and 610 nm emission filters.

2.7. Mitochondrial membrane potential

Mitochondria membrane potential was evaluated using the lipophilic cationic probe JC-1 (Invitrogen) according to the manufacturer's instruction. Cells were harvested and resuspended in PBS. After adding 2 μM JC-1, cells were incubated for 30 min at 37 °C with rotation. Cells were washed with PBS and analyzed by flow cytometry (Becton Dickinson) using 488 nm excitation with emission filters appropriate for 515 nm and 580 nm.

2.8. Confocal microscopy

After being treated with cystamine or cysteamine for 72 h, cells were washed with cold PBS. The cells were fixed with 4% formaldehyde in PBS for 15 min at room temperature, and then permeabilized with 0.1% Triton X-100 in PBS for 5 min at room temperature followed by blocking with 1% BSA in PBST (PBS containing 0.1% Tween-20) for 30 min. AIF was labeled by an anti-AIF antibody (Santa Cruz Biotechnology) diluted in PBST and fluorescently labeled by 20 μg/ml of FITC-conjugated goat anti-mouse IgG (Molecular Probes, Eugene, OR, USA) in PBS containing 1% BSA for 1 h. Nucleus was labeled by 1 μg/ml of DAPI (Roche, Mannheim, Germany) in the solution. A confocal fluorescence microscope (LSM 510 META; Carl Zeiss, Oberkochen, Germany) was used to visualize the each sample.

2.9. Caspase-3-like and caspase-9-like activity assay

Caspase activity was measured by using chromogenic substrates, Ac-DEVD-pNA for caspase-3-like activity and Ac-LEHD-pNA for caspase-9-like activity (A.G. Scientific Inc., San Diego, CA, USA), as previously described with minor modification [32]. Cells were harvested and lysed in buffer (50 mM HEPES, pH 7.4, 0.1% CHAPS, 1 mM DTT, 0.1 mM EDTA and 0.1% Triton X-100) for 30 min followed by centrifugation at 12000 *g* for 10 min at 4 °C. The protein concentration in the supernatant was quantitated by the BCA method (Pierce). The cell extract (50 μg of protein) was added to assay buffer (100 mM HEPES, pH 7.4, 0.1% CHAPS, 10 mM DTT, 10% glycerol and 2% (v/v) DMSO) containing 2 mM chromogenic substrates and incubated for 4 h at 37 °C. Caspase activity was quantified by measuring the absorbance at 405 nm on microplate spectrophotometer. Caspase activity is calculated as described in the protocol for the CaspACE™ Assay System Kit (Promega) and each treatment was assessed as a percentage of the untreated control values.

2.10. Western blot analysis

Cells were sonicated in buffer (50 mM Tris–Cl, pH 7.4, 150 mM NaCl, 1% Triton X-100, protease inhibitor cocktail (Roche) and phosphatase inhibitor cocktail (Roche)) and centrifuged 20000 *g* for 10 min at 4 °C. After determination of protein concentration in the cell extract by the BCA method, 40 μg of protein was resolved by SDS-PAGE and transferred to a nitrocellulose membrane. Membranes were blocked for 1 h with 5% skim milk in Tris-buffered saline, and incubated with anti-TG2 [33], anti-AIF (Santa Cruz Biotechnology), anti-GCS_C (catalytic subunit of GCS; Santa Cruz Biotechnology) and anti-Actin (Sigma-Aldrich Corporation) antibodies. The membranes were washed and incubated with horseradish peroxidase-conjugated secondary antibody, followed by enhanced chemiluminescence development according to the manufacturer's instruction (Pierce).

2.11. Measurement of glutathione concentration

GSH concentration was estimated by using a GSH assay kit (Cayman Chemical Co., Ann Arbor, MI, USA). Briefly, cells and tissues were lysed in buffer (50 mM Tris–Cl, pH 7.4, 150 mM NaCl, 1% Triton X-100), and centrifuged 10000 *g* for 15 min. After determination of protein concentration by the BCA method, cell lysates were subjected to sequential treatment of 5% (w/v) metaphosphoric acid (Sigma-Aldrich Corporation) and 0.1 M triethanolamine (Sigma-Aldrich Corporation). Deproteinized samples were mixed with a solution containing 5,5′-dithio-bis-2-nitrobenzoic acid (DTNB), and 5-thio-2-nitrobenzoic acid (TNB) produced by a reaction between the sulfhydryl groups of GSH and DTNB was estimated by measuring absorbance at 405 or 412 nm. Total GSH and oxidized GSH concentrations were determined after treatment of the samples with GSH reductase and 10 mM 2-vinylpyridine (Sigma-Aldrich Corporation), respectively. Reduced GSH was calculated by subtraction of oxidized GSH from total GSH.

2.12. Duodenal ulcer model in rat

All animal procedures were approved by the Institutional Animal Care and Use Committee at the Seoul National University College of Medicine (IACUC Approval No. SNU-130624-1). Duodenal ulcers were induced in female Sprague–Dawley rats aged 6–8 weeks (Orient, Seoul, Korea) by intragastric administration of cysteamine as previously reported [34]. Cysteamine (25 mg/100 g body weight, Sigma-Aldrich Corporation) was given three times at 4 h intervals. Rats were euthanized at 10 or 24 h after the first dose of cysteamine and duodenums were collected for estimation of GSH content and immunofluorescence staining.

2.13. Statistical analysis

All statistical calculations were performed using Prism 4.0 (GraphPad, San Diego, CA, USA). Differences between two variables and multiple variables were assessed by unpaired Student's *t* test and one-way ANOVA with Tukey's multiple comparison test, respectively. The difference was considered significant if the *p* value was less than 0.05.

3. Results

3.1. Cystamine and cysteamine induce tumor cell-type specific cell death

To evaluate cystamine toxicity, we treated the DU145, HeLa, MCF7 and A549 cell lines with various cystamine concentrations for 72 h. Interestingly, we discovered that cystamine treatment resulted in a dose- and time-dependent cytotoxicity in the DU145 and HeLa cell lines but showed no effect in the MCF7 and A549 cell lines (Fig. 1a–d). In addition, neuroblastoma cells (SK-N-SH and SH-SY-5Y) were also resistant to cystamine treatment (Fig. 1e). Cystamine is reduced into two cysteamine molecules in the cytosol. To determine whether the cytotoxicity was caused by cystamine or its reduced form cysteamine, we also evaluated cysteamine toxicity in DU145 cells. Both MTT and LDH release assays demonstrated that cysteamine also induced cell death in a dose-dependent manner, and half of the cystamine dose was required to induce a similar rate of cell death compared to cysteamine-treated cells (Fig. 1f, g), indicating that cysteamine is responsible for cell type-specific cytotoxicity.

3.2. Cystamine cytotoxicity is not associated with unfolded protein response, ROS generation or TG2 activity

We investigated the mechanisms for cystamine cytotoxicity. Cysteamine is a reducing agent that could induce cell death by eliciting unfolded protein response [35]. To test this possibility, we examined the

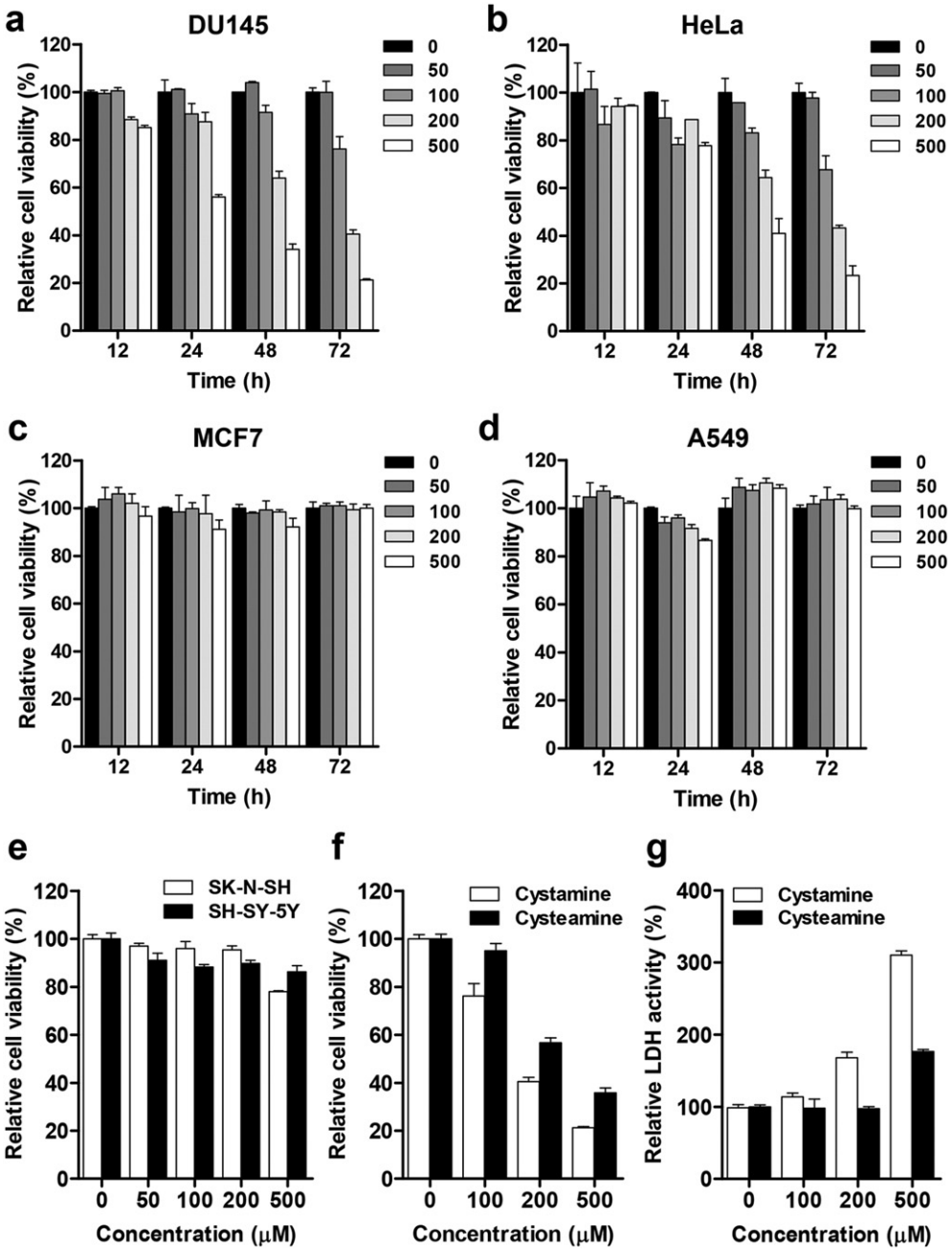

Fig. 1. Cell-type specific cystamine cytotoxicity. (a–d) DU145 (a), HeLa (b), MCF7 (c) and A549 (d) cells were treated with various cystamine concentrations (0–500 μM). Cell viability was monitored for 72 h using an MTT assay. (e) Neuroblastoma cells (SK-N-SH and SH-SY-5Y) were treated with cystamine for 72 h. Cell viability was measured by MTT assay. (f, g) DU145 cells were treated with cystamine or cysteamine for 72 h. Cell viability was measured by MTT assay (e) and LDH release assay (f). The data represent the mean values ± standard deviations based on experiments that were performed in triplicate.

sensitivity of cell lines to DTT and β-ME. There was no significant difference in cell viability among the cystamine-sensitive and -resistant cells (Fig. 2a, b), indicating that cystamine cytotoxicity is not caused by unfolded protein response.

Cysteamine produces H_2O_2 by reaction of the thiol group with metal ions [36]. To assess this possibility, we measured ROS levels in DU145 cells using DCF dye. Cystamine or cysteamine treatment reduced, rather than increased, fluorescence intensity (Fig. 2c). Antioxidants such as vitamin C, vitamin E, Trolox and quercetin had no effect on cystamine toxicity. Interestingly, only NAC abrogated cystamine toxicity (Fig. 2d). Moreover, exogenous H_2O_2 was more toxic to MCF7 and A549 cells than DU145 and HeLa cells (data not shown), and addition of polyethylene glycol (PEG)-conjugated catalase had little effect on cystamine sensitivity (Fig. 2e), suggesting that H_2O_2 generation did not contribute to cystamine cytotoxicity.

TG2 suppresses oxidative stress-induced apoptosis through cross-linking of caspase-3 and IκB [37], and cystamine inhibits TG2 by a thiol–disulfide exchange reaction [36]. To test whether TG2 might

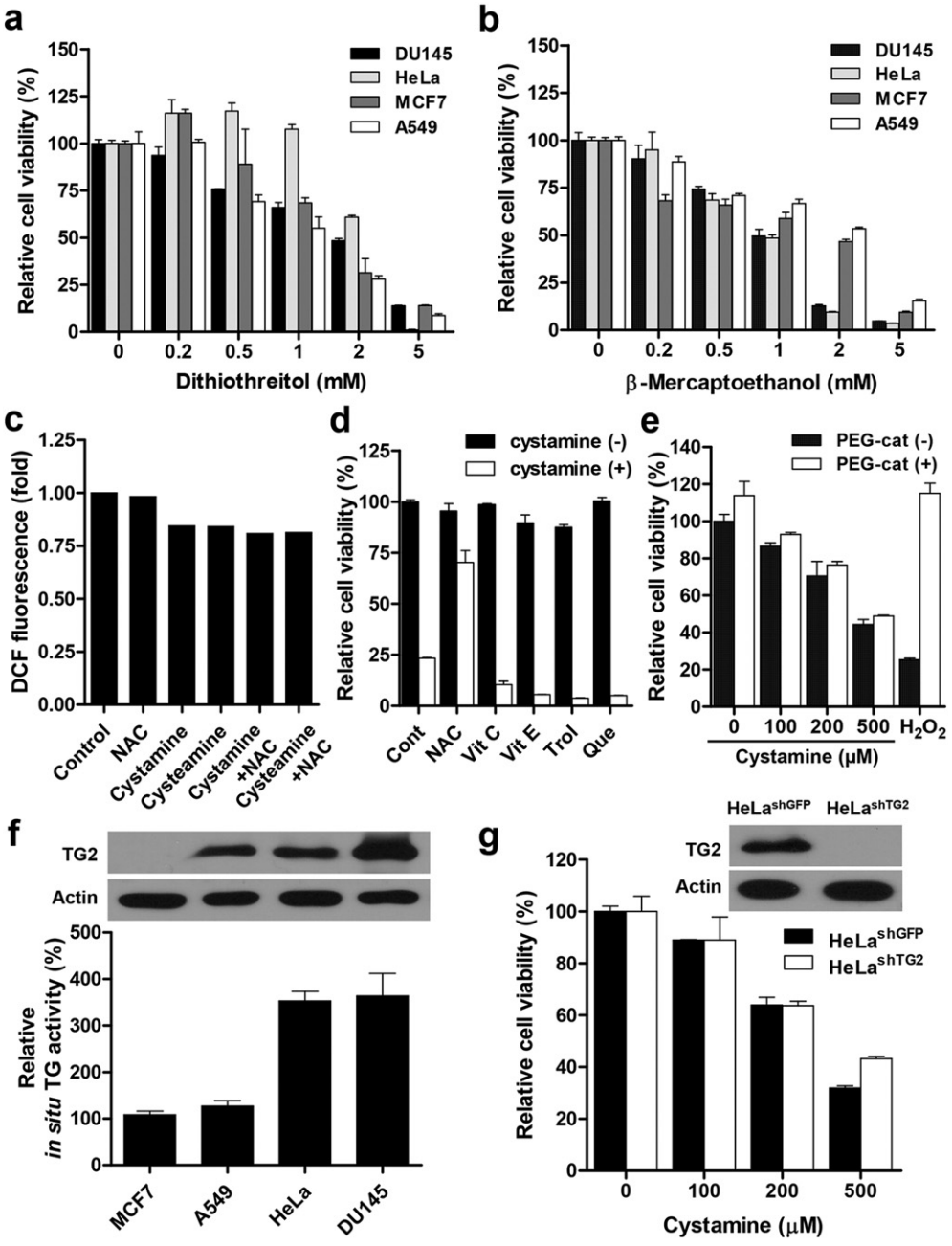

Fig. 2. Cystamine-induced cell death is not associated with unfolded protein response, ROS generation and transglutaminase 2 (TG2) activity. (a, b) DU145, HeLa, MCF7 and A549 cells were treated with dithiothreitol (0–5 mM, a) or β-mercaptoethanol (0–5 mM, b) for 72 h, and cell viability was examined using an MTT assay. (c) DU145 cells were treated with cystamine (500 μM) or cysteamine (1000 μM) in the presence of N-acetylcysteine (NAC, 500 μM) for 72 h. Cellular ROS levels were estimated by flow cytometry using the ROS-sensitive fluorescence dye DCF. The graph represents the mean values. (d) DU145 cells were treated with cystamine (500 μM) for 72 h in the presence of NAC (2 mM), vitamin C (Vit C; 2 mM), vitamin E (Vit E; 200 μM), Trolox (Trol; 1 mM) or quercetin (Que; 10 μM). Cell viability was assessed by an MTT assay. (e) DU145 cells were treated with cystamine (0–500 μM) for 72 h in the presence of polyethylene glycol (PEG)-conjugated catalase (PEG-cat; 500 U/ml). Cell viability was assessed by an MTT assay. H_2O_2 (1 mM)-treated cells were used as positive controls for the effect of PEG-conjugated catalase. (f) TG2 protein levels and *in situ* TG activity in DU145, HeLa, MCF7 and A549 cells was measured by Western blot analysis and a 5-biotinamidopentylamine incorporation assay, respectively. (g) HeLa cells were transfected with either shTG2 expression vector ($HeLa^{shTG2}$) or control vector ($HeLa^{shGFP}$). Cell viability was assessed after cystamine (0–500 μM) treatment for 72 h using an MTT assay. The protein levels of TG2 and actin were determined by Western blot analysis. The data represent the mean values ± standard deviations based on experiments that were performed in triplicate.

participate in cystamine toxicity, we compared TG2 protein levels and its intracellular activity among cell lines. TG2 expression levels were variable and not correlated with cystamine sensitivity (Fig. 2f). *In situ* TG activity in DU145 and HeLa cells was higher than that in MCF7 and A549 cells (Fig. 2f), and down-regulation of TG2 by shRNA in HeLa cells had no effects on cystamine sensitivity (Fig. 2g). These results indicate that cystamine cytotoxicity was not due to TG2 activity inhibition.

3.3. Cystamine-induced cell death depends on intracellular GSH levels

Cystamine treatment decreases cellular GSH level through GCS inhibition [2,19]. We therefore speculated that cell-type specific cystamine-induced cell death may be explained by a difference in the ability of the cells to synthesize GSH. To test this hypothesis, we monitored GSH levels. Upon cystamine treatment, total and reduced GSH levels in cystamine-sensitive cells (DU145 and HeLa) were maintained for 24 h but decreased thereafter. In contrast, GSH levels in cystamine-resistant cells (MCF7 and A549) were increased approximately 1.8- to 2.2-fold after 24 h, and basal GSH levels were maintained even in the presence of cystamine (Fig. 3a, b), demonstrating that GSH levels are well correlated with cystamine susceptibility. We next assessed whether GCS protein levels are important in regulating intracellular GSH levels. Western blot analysis revealed that in cystamine-sensitive cells, GCS levels were increased during the initial 24 h of cystamine treatment, but decreased abruptly after 48 or 72 h (Fig. 3c), whereas in cystamine-resistant cells, basal GCS levels were maintained for 72 h (Fig. 3d), indicating that GCS expression is correlated with intracellular GSH levels and a major determinant of cystamine sensitivity.

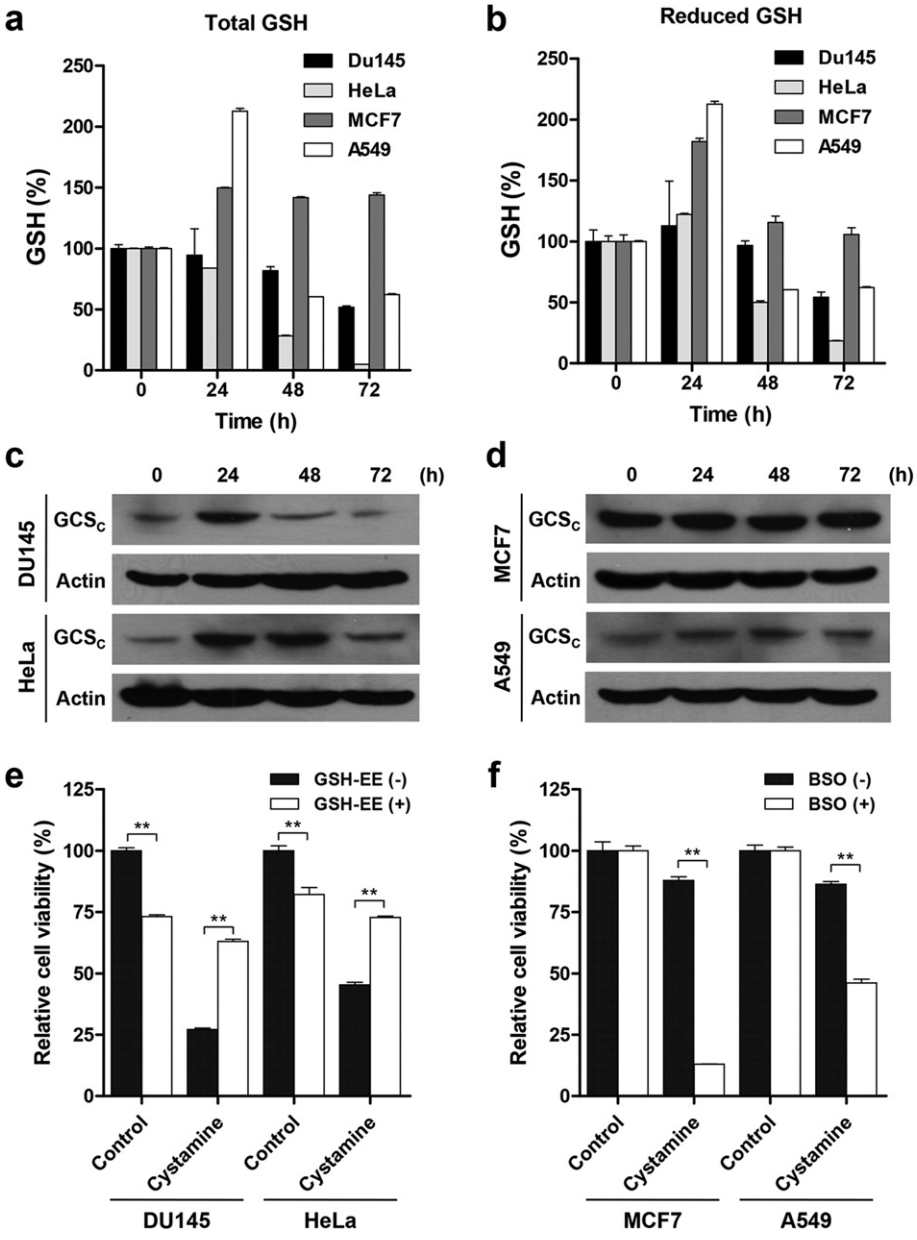

Fig. 3. Cystamine depletes intracellular glutathione levels in a cell-type specific manner. (a, b) DU145, HeLa, MCF7 and A549 cells were treated with cystamine (500 μM). Total (a) and reduced (b) GSH levels were monitored for 72 h. The GSH levels were expressed as a percentage of untreated control in each cell line. The data represent the mean values ± standard deviations based on experiments that were performed in triplicate. (c, d) γ-Glutamylcysteine synthetase catalytic subunit (GCS_C) expression was evaluated after cystamine treatment by Western blot analysis in cystamine-sensitive cells (DU145 and HeLa, c) and cystamine-resistant cells (MCF7 and A549, d). (e, f) Cystamine-sensitive cells (DU145 and HeLa, e) and cystamine-resistant cells (MCF7 and A549, f) were treated with glutathione ethyl ester (GSH-EE, 2.5 mM, e) and buthionine sulfoximine (BSO, 200 μM, f), respectively. Cell viability after cystamine (500 μM) treatment was monitored by MTT assay. The data represent the mean values ± standard deviations based on experiments that were performed in triplicate. Asterisks indicate statistically significant differences ($^{**}p < 0.01$) according to GSH-EE or BSO treatment.

We asked whether augmenting intracellular GSH levels could prevent cystamine-induced cell death. In cystamine-treated DU145 and HeLa cells, GSH-EE supplementation completely rescued cystamine-induced cell death (Fig. 3e). Conversely, GSH synthesis inhibition by BSO treatment rendered MCF7 and A549 cells cystamine-sensitive (Fig. 3f), demonstrating that GSH depletion is critical for triggering cell death.

3.4. Cystamine induces caspase-independent cell death

To gain insight into the mechanisms of cystamine cytotoxicity, we investigated the morphological and biochemical features of cystamine-induced cell death [38]. We examined the effect of cystamine on DNA fragmentation by staining with propidium iodide. Flow cytometric analysis revealed that cystamine treatment resulted in

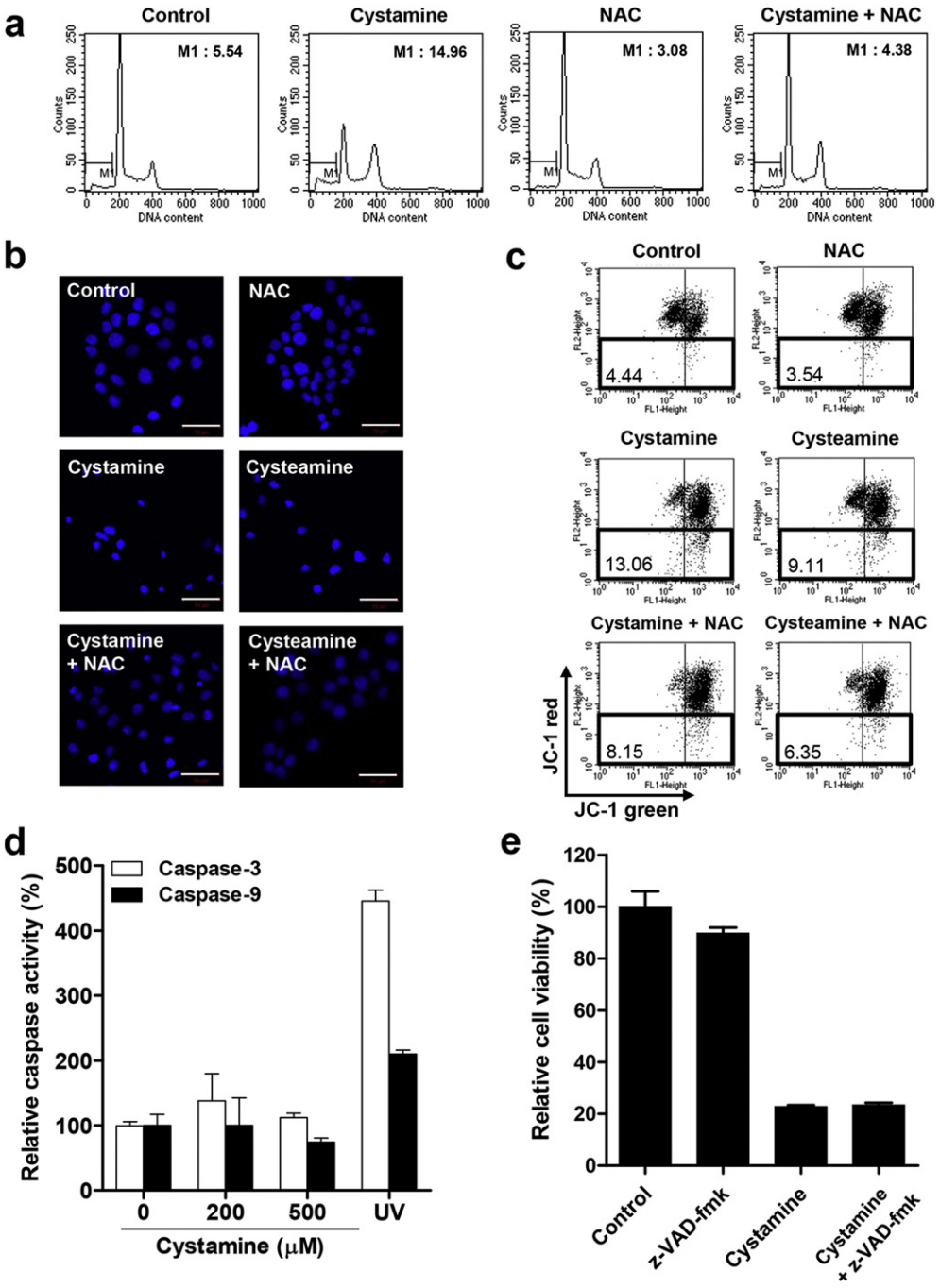

Fig. 4. Cystamine treatment induces caspase-independent apoptosis. (a) Representative examples of flow cytometry profiles from cystamine (500 μM) and/or NAC (500 μM)-treated HeLa cells after 72 h of treatment. Cells were stained with propidium iodide. M1 represents the percentage of cells containing sub-G1 DNA content. (b) Representative DAPI-stained cystamine (500 μM) or cysteamine (1000 μM)-treated HeLa cells in the presence of NAC (500 μM). Scale bar: 50 μm. (c) Cells were treated with cystamine (500 μM) or cysteamine (1000 μM) for 72 h. Mitochondrial membrane potential was analyzed by flow cytometry using JC-1 dye. The number in each graph indicates the relative percentage of cells with reduced red fluorescence. (d) Caspase-3-like and -9-like activities were measured after cystamine (200 and 500 μM) treatment using Ac-DEVD-pNA and Ac-LEHD-pNA as substrates, respectively. Caspase-3-like and -9-like activities after ultraviolet (UV) irradiation were used as positive controls. (e) Cell viability after cystamine (500 μM) treatment for 72 h in the presence of z-VAD-fmk (10 μM) was assessed using an MTT assay. The data represent the mean values ± standard deviations based on experiments that were performed in triplicate.

approximately a 3-fold increase of the SubG1 fraction in DU145 cells compared with control cells (Fig. 4a). When stained with DAPI, cystamine- or cysteamine-treated cells displayed condensed chromatin compared with control cells (Fig. 4b). Moreover, cystamine or cysteamine evoked mitochondrial membrane depolarization (Fig. 4c). These features were prevented by NAC (Fig. 4a–c). However, when caspase-3-like and -9-like activities were measured, we found no increase in either caspase activity in cystamine-treated cells (Fig. 4d). Furthermore, the caspase inhibitor z-VAD-fmk did not affect cystamine cytotoxicity (Fig. 4e), implying that cystamine-induced cell death is independent of caspase activity.

3.5. Cystamine induces AIF nuclear translocation in a cell-type specific manner

AIF is a mitochondrial flavoprotein that plays a major role in caspase-independent cell death [28]. Confocal microscopic analyses revealed that cystamine induced AIF nuclear translocation only in DU145 and HeLa cells, but not in MCF7 and A549 cells (Fig. 5a). Moreover, cystamine-induced AIF nuclear translocation was completely blocked by NAC (Fig. 5b). To further confirm the causal role of AIF in cystamine-induced cell death, we compared the cystamine cytotoxicity in wild-type and AIF-downregulated cells. AIF knockdown by siRNA

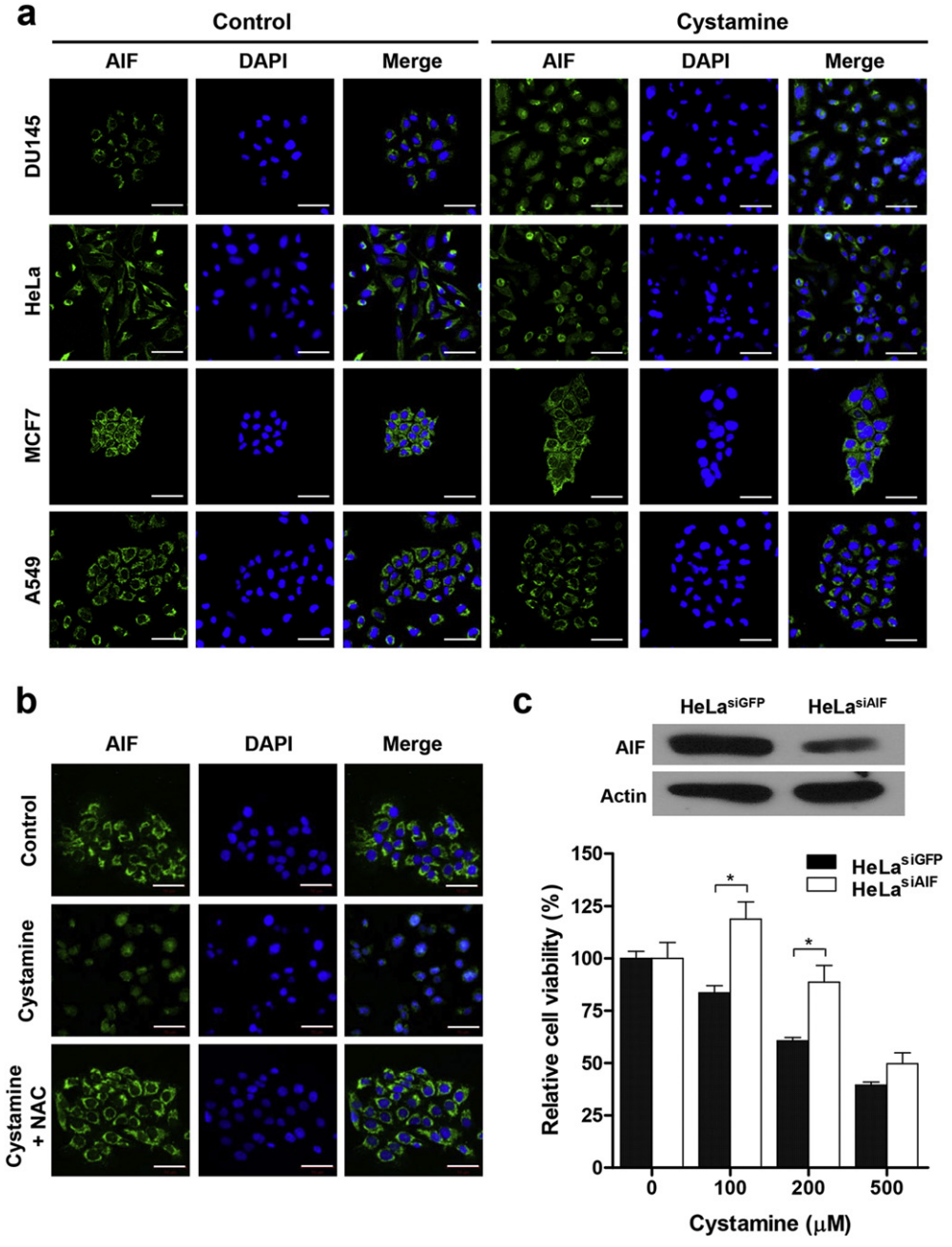

Fig. 5. Cystamine treatment triggers nuclear translocation of apoptosis-inducing factor (AIF). (a) AIF localization in cystamine-treated cells. DU145, HeLa, MCF7 and A549 cells were treated with cystamine (500 μM) for 72 h and immunostained with anti-AIF antibodies and FITC-conjugated goat anti-mouse IgG. AIF nuclear translocation was evaluated using confocal microscopy with DAPI staining. Scale bar: 50 μm. (b) DU145 cells were immunostained with anti-AIF antibodies and FITC-conjugated goat anti-mouse IgG in the presence of cystamine (500 μM) or NAC (500 μM). Scale bar: 50 μm. (c) Effect of AIF-knockdown on cystamine-induced cell death. HeLa cells were treated with AIF-specific siRNA. AIF protein levels and cell viability after cystamine treatment for 72 h were measured by Western blot analysis and MTT assay, respectively. The data represent the mean values ± standard deviations based on experiments that were performed in triplicate. Asterisks indicate statistically significant differences (*$p < 0.05$) compared with control siRNA-treated cells.

decreased the cell death in cystamine-treated cells, demonstrating an inverse relationship between AIF expression and cystamine cytotoxicity (Fig. 5c). These results indicate that cystamine induces cell death *via* AIF nuclear translocation.

We next tested the possibility that GSH depletion below a certain level may trigger AIF nuclear translocation. In cystamine-treated DU145 and HeLa cells, immunocytochemical staining demonstrated that GSH-EE treatment prevented cystamine-induced AIF nuclear translocation (Fig. 6), indicating that GSH depletion is critical for triggering AIF nuclear translocation.

3.6. Cystamine-induced AIF translocation is not associated with calpain I and PARP-1

Calpain I and poly (ADP-ribose) polymerase-1 (PARP-1) are involved in AIF nuclear translocation by various apoptogenic stimuli [28]. To assess whether these enzymes are also required for cystamine-induced AIF translocation, we treated DU145 and HeLa cells with the calpain inhibitor ALLN or the PARP-1 inhibitor DPQ (3,4-dihydro-5-[4-(1-piperidinyl)butoxy]-1(2H)-isoquinolinone), and we found that these enzyme inhibitors had no effect on cystamine-induced cell death in both cell lines (Fig. 7a, b), suggesting that GSH depletion might be a new pathway for promoting AIF nuclear translocation.

3.7. Cysteamine induces AIF-mediated apoptosis in a rat model of duodenal ulcer

We next sought to extend these results from cellular models to an *in vivo* model of cysteamine toxicity. In rat, cysteamine is a well-known chemical to induce perforating duodenal ulcer in the proximal duodenum after 24–48 h of administration [20,34]. We tested whether intragastric administration of cysteamine could induce apoptosis of duodenal epithelial cells by depleting GSH and triggering AIF nuclear translocation. Female Sprague–Dawley rats received cysteamine (25 mg/100 g body weight) three times at 4 h intervals. Duodenal ulcer was developed within 48 h in all animals receiving cysteamine. When GSH levels were determined in the duodenal tissues, total GSH concentrations were decreased after 10 h which were restored after 24 h of cysteamine administration (Fig. 8a). Concurrently, immunofluorescence staining of AIF revealed that AIF was translocated into the nucleus of duodenal epithelium after 24 h of cysteamine administration (Fig. 8b), indicating that AIF translocation caused by GSH depletion may be a relevant molecular mechanism for cysteamine-induced duodenal ulcer in rat.

4. Discussion

In the present study, we investigated cystamine toxicity and found that cystamine induced caspase-independent cell death in a cell type-specific manner. Comparison between cystamine-sensitive and -resistant cells demonstrated that cystamine-induced cell death is caused by AIF nuclear translocation. Subsequent analyses identified the decreased GSH levels as a triggering factor for AIF translocation. A causal role of GSH depletion is demonstrated by the observations that GSH supplementation completely prevented AIF nuclear translocation. Moreover, these results from cellular models were verified in a rat model of cysteamine-induced duodenal ulcer. Our data also demonstrated that cystamine cytotoxicity is not associated with its ability to induce unfolded protein response, to generate ROS, or to inhibit TG2 activity. Collectively, our results indicate that AIF nuclear translocation induced by GSH depletion is a critical molecular event in cystamine toxicity.

Cysteamine is an intracellular reduced form of cystamine and is synthesized from pantetheine by membrane-anchored pantetheinase, an enzyme encoded by the widely expressed vanin gene family. Cysteamine is catabolized to hypotaurine and taurine by cysteamine dioxygenase [18,39]. The concentrations of cystamine and cysteamine in brain and plasma are very low (under the detection limit) [40], and the molecular mechanism of transport of cystamine and cysteamine into cells has not been revealed yet. Although cysteamine is an aminothiol that could act as an antioxidant scavenging hydroxyl radical, hypochlorous acid and hydrogen peroxide [4], the physiological role of cysteamine remains unknown because conflicting evidences of its role in redox regulation have been reported. Administration of cystamine showed rapid cleavage into two cysteamine molecules and an increase of the cellular antioxidant L-cysteine in mouse model of Huntington's disease [1,41] and GSH levels particularly in neuronal cells and tissues in mouse [3,42]. On the other hand, pantetheinase-deficient mice exhibited higher GSH production, suggesting an inhibitory role of cysteamine in GSH synthesis [6]. Consistent with these results, our data demonstrated that cysteamine treatment suppresses cellular GSH production in rat duodenal epithelial cells as well as in specific cell-lines, indicating that intracellular GSH regulation is a critical determinant of cystamine cytotoxicity. Cysteamine is currently used to treat patients with nephropathic cystinosis. Recently, cystamine or cysteamine demonstrated beneficial effects in mouse models of Huntington's disease [8], Parkinson's disease [10], selenite-induced cataract formation [39] and bleomycin-induced lung fibrosis [43]. The results described here suggest that these effects of cystamine should be carefully re-evaluated after long-term administration.

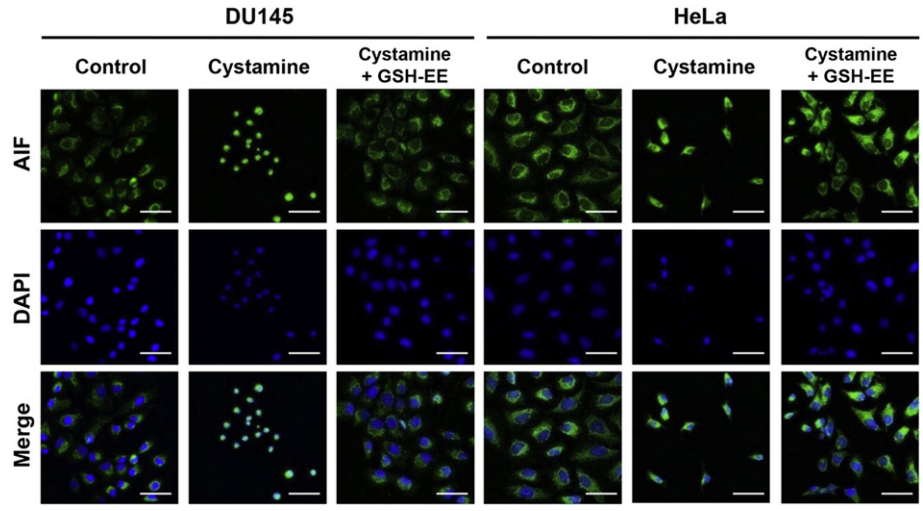

Fig. 6. Cystamine-induced AIF translocation depends on intracellular GSH levels. DU145 and HeLa cells were treated with GSH-EE (2.5 mM) and cystamine (500 μM) and immunostained with anti-AIF antibodies and FITC-conjugated goat anti-mouse IgG. Scale bar: 50 μm.

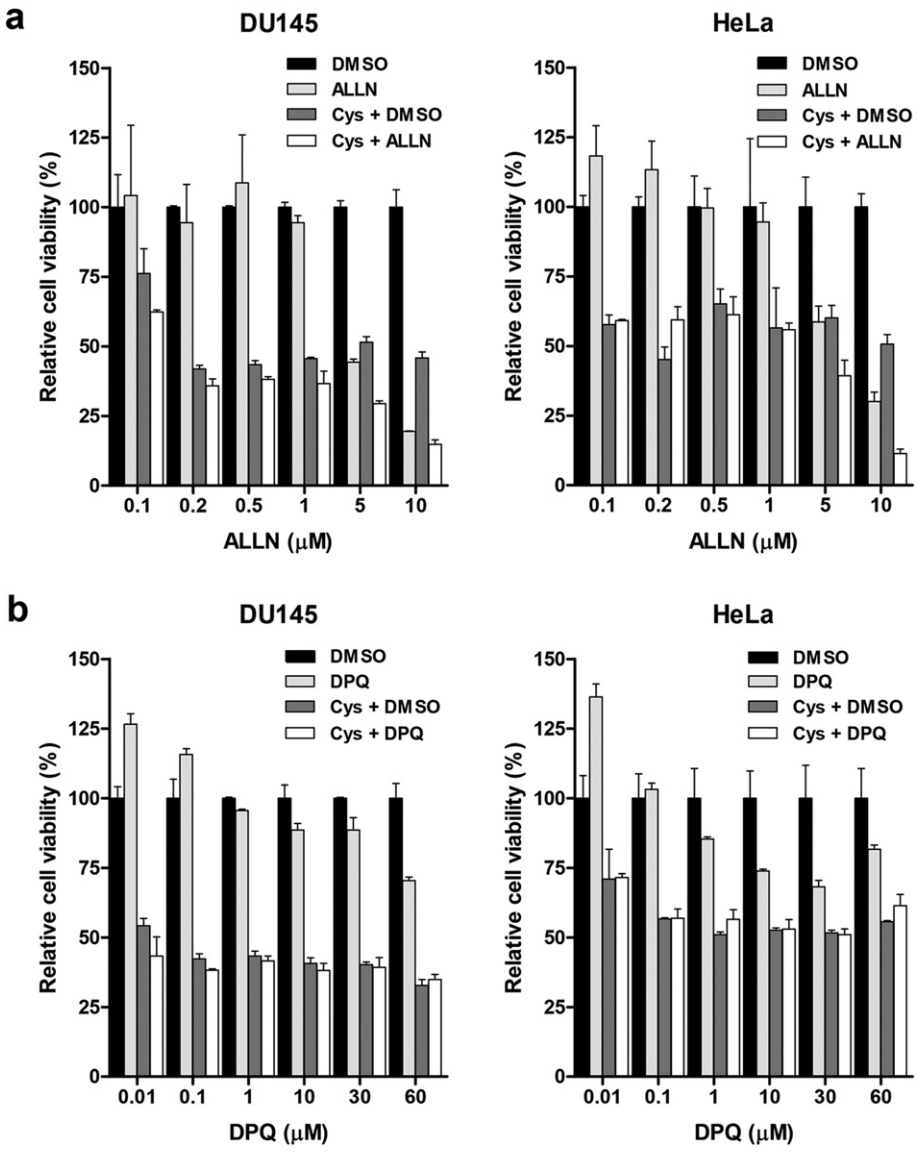

Fig. 7. Effect of inhibitors for calpain or poly (ADP-ribose) polymerase-1 (PARP-1) on cystamine cytotoxicity. (a, b) DU145 and HeLa cells were treated with cystamine (Cys, 500 μM) in the presence of calpain inhibitor ALLN (0.1–10 μM, a) or PARP-1 inhibitor DPQ (0.01–60 μM, b) for 72 h. Cell viability was measured by MTT assay. Dimethyl sulfoxide (DMSO)-treated cells were used as control for inhibitors. The data represent the mean values ± standard deviations based on experiments that were performed in triplicate.

Intracellular GSH levels are modulated in multiple ways. At the transcriptional level, cellular GSH content is strictly regulated by GCS expression levels. GCS is a heterodimer that is composed of a catalytic (GCS_C) and modifier subunit (GCS_M). GCS_C transcription is regulated by TPA and an electrophile response element, which are activated by AP-1 and Nrf2, respectively [21]. Cystamine treatment reportedly activated Nrf2 pathway both in cell culture and in brain tissue [42]. At the enzyme level, GCS_C activity is increased by GCS_M in response to oxidative insults, but is inhibited by GSH *via* negative feedback [44]. Moreover, GCS_C is inhibited by cellular metabolite cysteamine through a sulfhydryl–disulfide interchange reaction between GCS_C and cysteamine *in vitro* and *in vivo* [2,6]. Thus, the decreased GCS_C activity and expression in cystamine-treated cells as demonstrated in this study suggest that cystamine functions as a negative regulator to limit GSH production, which modulates cellular responses to external stress. Although NAC replenishes intracellular GSH by providing cysteine, the protective effect of NAC in cystamine cytotoxicity is probably attributed to a direct adduct formation and interference with cystamine, or substitute for the functions of GSH through its sulfhydryl group. In addition, our data also suggest that aberrant regulation of GSH level may contribute to the defective triggering of AIF nuclear translocation in response to various apoptotic stimuli. Therefore, regulation of intracellular GSH levels is an important point of control in AIF-mediated caspase-independent cell death.

AIF is an oxidoreductase located in the mitochondrial inner membrane which is essential for maintenance of the mitochondrial respiratory chain complex I and redox status [45]. AIF also mediates caspase-independent cell death in response to alkylating agents, excitotoxins, hypoxia/ischemia and growth factor deprivation [28]. Our data demonstrated that GSH depletion triggers AIF nuclear translocation even in the absence of oxidative stress, indicating that GSH depletion is a downstream signal linking apoptotic stimuli with AIF nuclear translocation, but is not a simple marker of oxidative stress in the caspase-independent cell death. In support of this notion, increased export of cellular GSH has been observed in AIF-mediated cell death induced by treatment with glutamate, N-methyl-D-aspartate, kainate, and hypoxia/ischemia [46–48]. Moreover, our results also showed decreased total GSH in the cysteamine-treated duodenal mucosal cells in rats. These observations suggest that increased GSH efflux likely contributes to GSH depletion causing AIF-mediated cell death. Because GSH efflux is an

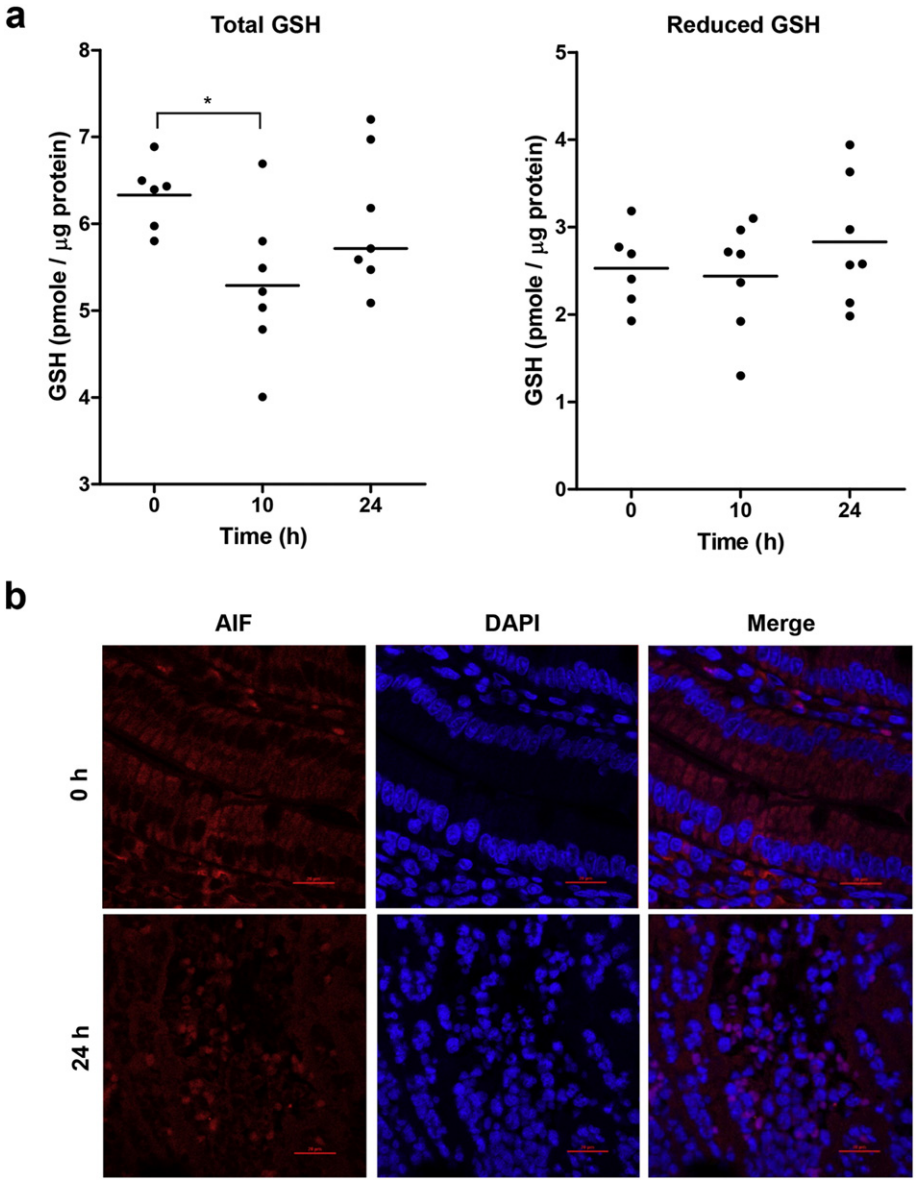

Fig. 8. Cysteamine induces AIF-mediated apoptosis through GSH depletion in a rat model of duodenal ulcer. (a) Total and reduced GSH levels in the proximal duodenal tissues after cysteamine administration. Duodenal ulcers were induced in female Sprague–Dawley rats by intragastric cysteamine administration. Three doses of cysteamine (25 mg/100 g body weight each time) were given at 4 h intervals, and GSH levels were estimated 10 and 24 h after the first dose of cysteamine. Asterisk indicates statistically significant difference (*$p < 0.05$). (b) AIF localization in cysteamine-treated rat duodenum. After cysteamine administration, duodenal tissues were immunostained with anti-AIF antibodies and FITC-conjugated goat anti-mouse IgG, and nuclei were counter-stained with DAPI. Scale bar: 20 μm.

active process regulating cellular redox homeostasis, GSH transporters such as multidrug resistance proteins, the organic anion transporter and the glutamate/aspartate transporter might play an important role in modulation of AIF-mediated cell death [49]. Thus, it will be of interest to elucidate the role of GSH transporters in AIF translocation that is induced by chemicals associated with cellular redox status and GSH level alterations including As_2O_3, cladribine, granulysin, geldanamycin, staurosporine, sulindac, camptothecin, hexaminolevulinate and DNA alkylating agents [28]. Moreover, GSH depletion is also required for caspase activation, apoptosome formation and cytosolic cytochrome *c* release, most likely through redox-based protein modifications such as glutathionylation and nitrosylation [22]. Therefore, GSH depletion may be involved in the regulation of caspase-independent and -dependent apoptosis.

The *Harlequin* (*Hq*) mouse is a strain that harbors an AIF gene insertion mutation resulting in an 80% reduction of AIF expression. *Hq* mice exhibited protection from ischemia-induced brain damage, and primary neuronal cells were resistant to hypoxia/ischemia-induced cell death [50–52]. However, *Hq* mice paradoxically developed age-associated cerebellum and retinal degeneration with increased lipid peroxide and 8-hydroxydeoxyguanine levels [22], and cultured cerebellar granule cells from *Hq* mice were more sensitive to ROS-induced cell death than those from wild-type mice [53]. Our results may provide a molecular explanation for these contradictory phenotypes of *Hq* mice. We demonstrated that AIF-mediated cell death occurred under GSH-depleted conditions, suggesting that AIF functions as an eliminator of cells with low GSH content. Therefore, AIF-knockdown cells could survive even in low GSH levels in which wild-type cells undergo cell death, but these cells subsequently become dysfunctional due to the accumulation of oxidatively damaged molecule. Moreover, the defective complex I function in AIF-knockdown cells may also contribute to increased oxidative stress. Interestingly, AIF protein levels in the cortical

area of normal human brains reportedly increased with aging, but was lower in cortical brains from Alzheimer's disease patients compared with age-matched controls [54], suggesting a role for AIF in the pathogenesis of neurodegenerative disease. However, further studies would be required to establish the cause-result relationship between AIF expression and neurodegeneration.

In summary, we demonstrated that cystamine-induced GSH depletion caused cell death by triggering AIF nuclear translocation in cellular and animal models. This is the first report on the molecular mechanism of cystamine toxicity and provides important implications for cystamine in neurodegenerative disease therapeutics. In addition, our data indicate that GSH may play a role in the regulation of AIF-mediated cell death as well as in the maintenance of redox homeostasis in response to oxidative stress. These results may provide new insights into the pathophysiological role of cysteamine, GSH and AIF in various diseases.

Acknowledgement

This work was supported by grants from the National Research Foundation of Korea (NRF-2010-0014684, 2010-0019472, and 2012R1A1A2005188) and the Korea Healthcare Technology R&D project, Ministry of Health and Welfare (grant No. A100190). S.Y.C., J.H.L. and H.J.K. were supported by the second phase of the Brain Korea 21 Program (5262-20140100).

References

[1] J.H. Fox, D.S. Barber, B. Singh, B. Zucker, M.K. Swindell, F. Norflus, R. Buzescu, R. Chopra, R.J. Ferrante, A. Kazantsev, S.M. Hersch, Cystamine increases L-cysteine levels in Huntington's disease transgenic mouse brain and in a PC12 model of polyglutamine aggregation, J. Neurochem. 91 (2004) 413–422.
[2] O.W. Griffith, A. Larsson, A. Meister, Inhibition of gamma-glutamylcysteine synthetase by cystamine: an approach to a therapy of 5-oxoprolinuria (pyroglutamic aciduria), Biochem. Biophys. Res. Commun. 79 (1977) 919–925.
[3] M. Lesort, M. Lee, J. Tucholski, G.V. Johnson, Cystamine inhibits caspase activity. Implications for the treatment of polyglutamine disorders, J. Biol. Chem. 278 (2003) 3825–3830.
[4] O.I. Aruoma, B. Halliwell, B.M. Hoey, J. Butler, The antioxidant action of taurine, hypotaurine and their metabolic precursors, Biochem. J. 256 (1988) 251–255.
[5] T.M. Jeitner, E.J. Delikatny, J. Ahlqvist, H. Capper, A.J. Cooper, Mechanism for the inhibition of transglutaminase 2 by cystamine, Biochem. Pharmacol. 69 (2005) 961–970.
[6] F. Martin, M.F. Penet, F. Malergue, H. Lepidi, A. Dessein, F. Galland, M. de Reggi, P. Naquet, B. Gharib, Vanin-1(−/−) mice show decreased NSAID- and Schistosoma-induced intestinal inflammation associated with higher glutathione stores, J. Clin. Invest. 113 (2004) 591–597.
[7] A. Dedeoglu, J.K. Kubilus, T.M. Jeitner, S.A. Matson, M. Bogdanov, N.W. Kowall, W.R. Matson, A.J. Cooper, R.R. Ratan, M.F. Beal, S.M. Hersch, R.J. Ferrante, Therapeutic effects of cystamine in a murine model of Huntington's disease, J. Neurosci. 22 (2002) 8942–8950.
[8] M.V. Karpuj, M.W. Becher, J.E. Springer, D. Chabas, S. Youssef, R. Pedotti, D. Mitchell, L. Steinman, Prolonged survival and decreased abnormal movements in transgenic model of Huntington disease, with administration of the transglutaminase inhibitor cystamine, Nat. Med. 8 (2002) 143–149.
[9] E.C. Stack, J.L. Ferro, J. Kim, S.J. Del Signore, S. Goodrich, S. Matson, B.B. Hunt, K. Cormier, K. Smith, W.R. Matson, H. Ryu, R.J. Ferrante, Therapeutic attenuation of mitochondrial dysfunction and oxidative stress in neurotoxin models of Parkinson's disease, Biochim. Biophys. Acta 1782 (2008) 151–162.
[10] M.E. Tremblay, M. Saint-Pierre, E. Bourhis, D. Levesque, C. Rouillard, F. Cicchetti, Neuroprotective effects of cystamine in aged parkinsonian mice, Neurobiol. Aging 27 (2006) 862–870.
[11] S. Igarashi, R. Koide, T. Shimohata, M. Yamada, Y. Hayashi, H. Takano, H. Date, M. Oyake, T. Sato, A. Sato, S. Egawa, T. Ikeuchi, H. Tanaka, R. Nakano, K. Tanaka, I. Hozumi, T. Inuzuka, H. Takahashi, S. Tsuji, Suppression of aggregate formation and apoptosis by transglutaminase inhibitors in cells expressing truncated DRPLA protein with an expanded polyglutamine stretch, Nat. Genet. 18 (1998) 111–117.
[12] T.C. Hsu, Y.C. Chen, W.X. Lai, S.Y. Chiang, C.Y. Huang, B.S. Tzang, Beneficial effects of treatment with cystamine on brain in NZB/WF1 mice, Eur. J. Pharmacol. 591 (2008) 307–314.
[13] R. Dubinsky, C. Gray, CYTE-I-HD: phase I dose finding and tolerability study of cysteamine (Cystagon) in Huntington's disease, Mov. Disord. 21 (2006) 530–533.
[14] R. Ientile, A. Campisi, G. Raciti, D. Caccamo, M. Curro, G. Cannavo, G. Li Volti, S. Macaione, A. Vanella, Cystamine inhibits transglutaminase and caspase-3 cleavage in glutamate-exposed astroglial cells, J. Neurosci. Res. 74 (2003) 52–59.
[15] M. Borrell-Pages, J.M. Canals, F.P. Cordelieres, J.A. Parker, J.R. Pineda, G. Grange, E.A. Bryson, M. Guillermier, E. Hirsch, P. Hantraye, M.E. Cheetham, C. Neri, J. Alberch, E. Brouillet, F. Saudou, S. Humbert, Cystamine and cysteamine increase brain levels of BDNF in Huntington disease via HSJ1b and transglutaminase, J. Clin. Invest. 116 (2006) 1410–1424.
[16] L. Di Leandro, B. Maras, M.E. Schinina, S. Dupre, I. Koutris, F.M. Martin, P. Naquet, F. Galland, G. Pitari, Cystamine restores GSTA3 levels in Vanin-1 null mice, Free Radic. Biol. Med. 44 (2008) 1088–1096.
[17] R.V. Lebo, N.M. Kredich, Inactivation of human gamma-glutamylcysteine synthetase by cystamine. Demonstration and quantification of enzyme–ligand complexes, J. Biol. Chem. 253 (1978) 2615–2623.
[18] G. Pitari, F. Malergue, F. Martin, J.M. Philippe, M.T. Massucci, C. Chabret, B. Maras, S. Dupre, P. Naquet, F. Galland, Pantetheinase activity of membrane-bound Vanin-1: lack of free cysteamine in tissues of Vanin-1 deficient mice, FEBS Lett. 483 (2000) 149–154.
[19] C. Berruyer, F.M. Martin, R. Castellano, A. Macone, F. Malergue, S. Garrido-Urbani, V. Millet, J. Imbert, S. Dupre, G. Pitari, P. Naquet, F. Galland, Vanin-1 −/− mice exhibit a glutathione-mediated tissue resistance to oxidative stress, Mol. Cell. Biol. 24 (2004) 7214–7224.
[20] S. Szabo, X. Deng, T. Khomenko, L. Chen, G. Tolstanova, K. Osapay, Z. Sandor, X. Xiong, New molecular mechanisms of duodenal ulceration, Ann. N. Y. Acad. Sci. 1113 (2007) 238–255.
[21] H.J. Forman, H. Zhang, A. Rinna, Glutathione: overview of its protective roles, measurement, and biosynthesis, Mol. Aspects Med. 30 (2009) 1–12.
[22] R. Franco, J.A. Cidlowski, Apoptosis and glutathione: beyond an antioxidant, Cell Death Differ. 16 (2009) 1303–1314.
[23] T.P. Dalton, Y. Chen, S.N. Schneider, D.W. Nebert, H.G. Shertzer, Genetically altered mice to evaluate glutathione homeostasis in health and disease, Free Radic. Biol. Med. 37 (2004) 1511–1526.
[24] J.S. Armstrong, K.K. Steinauer, B. Hornung, J.M. Irish, P. Lecane, G.W. Birrell, D.M. Peehl, S.J. Knox, Role of glutathione depletion and reactive oxygen species generation in apoptotic signaling in a human B lymphoma cell line, Cell Death Differ. 9 (2002) 252–263.
[25] C. Friesen, Y. Kiess, K.M. Debatin, A critical role of glutathione in determining apoptosis sensitivity and resistance in leukemia cells, Cell Death Differ. 11 (Suppl. 1) (2004) S73–S85.
[26] R. Franco, M.I. Panayiotidis, J.A. Cidlowski, Glutathione depletion is necessary for apoptosis in lymphoid cells independent of reactive oxygen species formation, J. Biol. Chem. 282 (2007) 30452–30465.
[27] N. Joza, J.A. Pospisilik, E. Hangen, T. Hanada, N. Modjtahedi, J.M. Penninger, G. Kroemer, AIF: not just an apoptosis-inducing factor, Ann. N. Y. Acad. Sci. 1171 (2009) 2–11.
[28] H.K. Lorenzo, S.A. Susin, Therapeutic potential of AIF-mediated caspase-independent programmed cell death, Drug Resist. Updat. 10 (2007) 235–255.
[29] M. Baritaud, H. Boujrad, H.K. Lorenzo, S. Krantic, S.A. Susin, Histone H2AX: the missing link in AIF-mediated caspase-independent programmed necrosis, Cell Cycle 9 (2010) 3166–3173.
[30] E. Daugas, S.A. Susin, N. Zamzami, K.F. Ferri, T. Irinopoulou, N. Larochette, M.C. Prevost, B. Leber, D. Andrews, J. Penninger, G. Kroemer, Mitochondrio-nuclear translocation of AIF in apoptosis and necrosis, FASEB J. 14 (2000) 729–739.
[31] S.Y. Cho, J.H. Lee, H.D. Bae, E.M. Jeong, G.Y. Jang, C.W. Kim, D.M. Shin, J.H. Jeon, I.G. Kim, Transglutaminase 2 inhibits apoptosis induced by calcium-overload through down-regulation of Bax, Exp. Mol. Med. 42 (2010) 639–650.
[32] J.J. Gu, K. Gathy, L. Santiago, E. Chen, M. Huang, L.M. Graves, B.S. Mitchell, Induction of apoptosis in IL-3-dependent hematopoietic cell lines by guanine nucleotide depletion, Blood 101 (2003) 4958–4965.
[33] J.H. Jeon, C.W. Kim, D.M. Shin, K. Kim, S.Y. Cho, J.C. Kwon, K.H. Choi, H.S. Kang, I.G. Kim, Differential incorporation of biotinylated polyamines by transglutaminase 2, FEBS Lett. 534 (2003) 180–184.
[34] T. Khomenko, J. Kolodney, J.T. Pinto, G.D. McLaren, X. Deng, L. Chen, G. Tolstanova, B. Paunovic, B.F. Krasnikov, N. Hoa, A.J. Cooper, S. Szabo, New mechanistic explanation for the localization of ulcers in the rat duodenum: role of iron and selective uptake of cysteamine, Arch. Biochem. Biophys. 525 (2012) 60–70.
[35] M. Csala, E. Margittai, G. Banhegyi, Redox control of endoplasmic reticulum function, Antioxid. Redox Signal. 13 (2010) 77–108.
[36] T.M. Jeitner, D.A. Lawrence, Mechanisms for the cytotoxicity of cysteamine, Toxicol. Sci. 63 (2001) 57–64.
[37] G.Y. Jang, J.H. Jeon, S.Y. Cho, D.M. Shin, C.W. Kim, E.M. Jeong, H.C. Bae, T.W. Kim, S.H. Lee, Y. Choi, D.S. Lee, S.C. Park, I.G. Kim, Transglutaminase 2 suppresses apoptosis by modulating caspase 3 and NF-kappaB activity in hypoxic tumor cells, Oncogene 29 (2010) 356–367.
[38] L. Galluzzi, I. Vitale, J.M. Abrams, E.S. Alnemri, E.H. Baehrecke, M.V. Blagosklonny, T.M. Dawson, V.L. Dawson, W.S. El-Deiry, S. Fulda, E. Gottlieb, D.R. Green, M.O. Hengartner, O. Kepp, R.A. Knight, S. Kumar, S.A. Lipton, X. Lu, F. Madeo, W. Malorni, P. Mehlen, G. Nunez, M.E. Peter, M. Piacentini, D.C. Rubinsztein, Y. Shi, H.U. Simon, P. Vandenabeele, E. White, J. Yuan, B. Zhivotovsky, G. Melino, G. Kroemer, Molecular definitions of cell death subroutines: recommendations of the Nomenclature Committee on Cell Death 2012, Cell Death Differ. 19 (2012) 107–120.
[39] S.M. Lee, E.M. Jeong, J. Jeong, D.M. Shin, H.J. Lee, H.J. Kim, J. Lim, J.H. Lee, S.Y. Cho, M.K. Kim, W.R. Wee, J.H. Lee, I.G. Kim, Cysteamine prevents the development of lens opacity in a rat model of selenite-induced cataract, Invest. Ophthalmol. Vis. Sci. 53 (2012) 1452–1459.
[40] J.T. Pinto, J.M. Van Raamsdonk, B.R. Leavitt, M.R. Hayden, T.M. Jeitner, H.T. Thaler, B.F. Krasnikov, A.J. Cooper, Treatment of YAC128 mice and their wild-type littermates with cystamine does not lead to its accumulation in plasma or brain: implications for the treatment of Huntington disease, J. Neurochem. 94 (2005) 1087–1101.
[41] M. Bousquet, C. Gibrat, M. Ouellet, C. Rouillard, F. Calon, F. Cicchetti, Cystamine metabolism and brain transport properties: clinical implications for neurodegenerative diseases, J. Neurochem. 114 (2010) 1651–1658.

[42] M.J. Calkins, J.A. Townsend, D.A. Johnson, J.A. Johnson, Cystamine protects from 3-nitropropionic acid lesioning via induction of nf-e2 related factor 2 mediated transcription, Exp. Neurol. 224 (2010) 307–317.
[43] K. Oh, H.B. Park, O.J. Byoun, D.M. Shin, E.M. Jeong, Y.W. Kim, Y.S. Kim, G. Melino, I.G. Kim, D.S. Lee, Epithelial transglutaminase 2 is needed for T cell interleukin-17 production and subsequent pulmonary inflammation and fibrosis in bleomycin-treated mice, J. Exp. Med. 208 (2011) 1707–1719.
[44] M. Tosic, J. Ott, S. Barral, P. Bovet, P. Deppen, F. Gheorghita, M.L. Matthey, J. Parnas, M. Preisig, M. Saraga, A. Solida, S. Timm, A.G. Wang, T. Werge, M. Cuenod, K.Q. Do, Schizophrenia and oxidative stress: glutamate cysteine ligase modifier as a susceptibility gene, Am. J. Hum. Genet. 79 (2006) 586–592.
[45] N. Vahsen, C. Cande, J.J. Briere, P. Benit, N. Joza, N. Larochette, P.G. Mastroberardino, M.O. Pequignot, N. Casares, V. Lazar, O. Feraud, N. Debili, S. Wissing, S. Engelhardt, F. Madeo, M. Piacentini, J.M. Penninger, H. Schagger, P. Rustin, G. Kroemer, AIF deficiency compromises oxidative phosphorylation, EMBO J. 23 (2004) 4679–4689.
[46] T.B. Garcia, K.R. Oliveira, J.L. do Nascimento, M.E. Crespo-Lopez, D.L. Picanco-Diniz, T.C. Mota, A.M. Herculano, Glutamate induces glutathione efflux mediated by glutamate/aspartate transporter in retinal cell cultures, Neurochem. Res. 36 (2011) 412–418.
[47] O. Orwar, X. Li, P. Andine, C.M. Bergstrom, H. Hagberg, S. Folestad, M. Sandberg, Increased intra- and extracellular concentrations of gamma-glutamylglutamate and related dipeptides in the ischemic rat striatum: involvement of glutamyl transpeptidase, J. Neurochem. 63 (1994) 1371–1376.
[48] C. Wallin, S.G. Weber, M. Sandberg, Glutathione efflux induced by NMDA and kainate: implications in neurotoxicity? J. Neurochem. 73 (1999) 1566–1572.
[49] R. Franco, J.A. Cidlowski, Glutathione efflux and cell death, Antioxid. Redox Signal. 17 (2012) 1694–1713.
[50] G. Cao, J. Xing, X. Xiao, A.K. Liou, Y. Gao, X.M. Yin, R.S. Clark, S.H. Graham, J. Chen, Critical role of calpain I in mitochondrial release of apoptosis-inducing factor in ischemic neuronal injury, J. Neurosci. 27 (2007) 9278–9293.
[51] C. Culmsee, C. Zhu, S. Landshamer, B. Becattini, E. Wagner, M. Pellecchia, K. Blomgren, N. Plesnila, Apoptosis-inducing factor triggered by poly(ADP-ribose) polymerase and Bid mediates neuronal cell death after oxygen-glucose deprivation and focal cerebral ischemia, J. Neurosci. 25 (2005) 10262–10272.
[52] C. Zhu, X. Wang, Z. Huang, L. Qiu, F. Xu, N. Vahsen, M. Nilsson, P.S. Eriksson, H. Hagberg, C. Culmsee, N. Plesnila, G. Kroemer, K. Blomgren, Apoptosis-inducing factor is a major contributor to neuronal loss induced by neonatal cerebral hypoxia–ischemia, Cell Death Differ. 14 (2007) 775–784.
[53] V. El Ghouzzi, Z. Csaba, P. Olivier, B. Lelouvier, L. Schwendimann, P. Dournaud, C. Verney, P. Rustin, P. Gressens, Apoptosis-inducing factor deficiency induces early mitochondrial degeneration in brain followed by progressive multifocal neuropathology, J. Neuropathol. Exp. Neurol. 66 (2007) 838–847.
[54] S. Reix, N. Mechawar, S.A. Susin, R. Quirion, S. Krantic, Expression of cortical and hippocampal apoptosis-inducing factor (AIF) in aging and Alzheimer's disease, Neurobiol. Aging 28 (2007) 351–356.